

Easy Ketimine Formation Assisted by Heteropolynuclear Gold–Thallium Complexes

Eduardo J. Fernández,^{*,§} Antonio Laguna,^{*,‡} José M. López-de-Luzuriaga,[§] Manuel Montiel,[§] M. Elena Olmos,[§] and Javier Pérez[§]

Departamento de Química, Universidad de la Rioja, Grupo de Síntesis Química de La Rioja, UA-CSIC, Complejo Científico Tecnológico, 26006 Logroño, Spain, and Departamento de Química Inorgánica, Instituto de Ciencia de Materiales de Aragón, Universidad de Zaragoza-CSIC, 50009 Zaragoza, Spain

Received December 2, 2005

Treatment of the heterometallic complexes $[\text{AuTl}(\text{C}_6\text{X}_5)_2(\text{L}^1)]$ ($\text{X} = \text{Cl}$ (**1a**), F (**1b**), $\text{L}^1 =$ ethylenediamine) with ketones at room temperature yields stable amine–imine or diimine complexes with the new ligands bound to the thallium centers. Besides their reactivity in solution, both amine complexes **1a** and **1b** react in the solid state with ketone vapors at room temperature in a few seconds.

Introduction

In the last years the synthesis of extended linear chain compounds has received renewed interest to chemists and physicists owing to their fascinating and unique chemical and physical properties.^{1,2} In fact, heterometallic systems have been shown as very promising candidates for photophysical studies³ that could lead to their use as light-emitting devices, and some of them can even be used as VOC sensors,^{4–11} but their utility as reagents for organic synthesis now appears as a new application for these systems. In this regard, nonconjugated diimines are tailored derivatives of bipyridine or phenanthroline-type organic ligands and used as a more flexible alternative to the conventional building blocks in supramolecular architectures,¹² in complexes with catalytic activity,¹³ in complexes that form supramolecular host–guest assemblies with electrical transport properties,¹⁴ or as stabilizing ligands of copper

photoluminescent chromophores.¹⁵ The classical synthesis of imines, originally reported by Schiff,¹⁶ involves a condensation of a carbonyl compound with an amine under azeotropic distillation¹⁷ to separate the liberated water. Usually, the reaction requires high temperatures, prolonged reaction periods, and the presence of external or in situ dehydrating agents in order to achieve better yields.^{18–21} Even the use of metal salts as catalysts or more specialized methods, as acids under microwave radiation or ionic liquids, have been reported.^{22–34} Even so, the efficiency of these procedures is limited to the reaction of highly electrophilic carbonyl compounds and strongly nucleophilic amines. In the particular case of ethylenediamine, the addition of acetone does not lead to the isolation of the corresponding diimine ligand because of its low stability. An alternative pathway consists of the coordination of ethylenediamine to the chosen metal center and the subsequent addition of the carbonyl-containing precursor. Nevertheless, the complexes prepared

* To whom the correspondence should be addressed. E-mail: alaguna@posta.unizar.es; eduardo.fernandez@dq.unirioja.es.

§ Universidad de la Rioja.

‡ Universidad de Zaragoza-CSIC.

(1) Hoffmann, R. *Angew. Chem., Int. Ed. Engl.* **1987**, *26*, 846.

(2) Williams, J. M.; Schultz, A. J.; Underhill, A. E.; Carneiro, K. *Extended Linear Chain Compounds*; Plenum Press: New York, 1982; Vols. 1–3.

(3) Fernández, E. J.; Laguna, A.; López-de-Luzuriaga, J. M. *Gold Bull.* **2001**, *34*, 14–19, and references therein.

(4) Beauvais, L. G.; Shores, M. P.; Long, J. R. *J. Am. Chem. Soc.* **2000**, *122*, 2763.

(5) Buss, C. E.; Mann, K. R. *J. Am. Chem. Soc.* **2002**, *124*, 1031.

(6) Cariati, E.; Bu, X.; Ford, P. C. *Chem. Mater.* **2000**, *12*, 3385.

(7) Dias, H. V.; Diyabalalage, H. V.; Rawashed-Omary, M.; Franzman, M. A.; Omary, M. A. *J. Am. Chem. Soc.* **2003**, *125*, 12072.

(8) Evju, J. K.; Mann, K. R. *Chem. Mater.* **1999**, *11*, 1425.

(9) Fernández, E. J.; López-de-Luzuriaga, J. M.; Monge, M.; Olmos, M. E.; Pérez, J.; Laguna, A.; Mohamed, A. A.; Fackler, J. P., Jr. *J. Am. Chem. Soc.* **2003**, *125*, 2022.

(10) Fernández, E. J.; López-de-Luzuriaga, J. M.; Monge, M.; Montiel, M.; Olmos, M. E.; Pérez, J.; Laguna, A.; Mendizábal, F.; Mohamed, A. A.; Fackler, J. P., Jr. *Inorg. Chem.* **2004**, *43*, 3573.

(11) Mansour, M. A.; Connick, W. B.; Lachicotte, R. J.; Gysling, H. J.; Eisenberg, R. *J. Am. Chem. Soc.* **1998**, *120*, 1329.

(12) Patra, G. K.; Goldberg, I. *Dalton Trans.* **2002**, 1051–1057.

(13) Schmid, M.; Eberhardt, R.; Kukral, J.; Rieger, B. *Z. Naturforsch.* **2002**, *1141*–1146.

(14) Pan, A.; Ghosh, A.; Chowdhury, S.; Datta, D. *Inorg. Chem. Commun.* **2001**, *4*, 507–510.

(15) Chowdhury, S.; Patra, G. K.; Drew, M. G. B.; Chattopadhyay, N.; Datta, D. *Dalton Trans.* **2000**, 235–237.

(16) Schiff, H. *Annals* **1864**, *131*, 118.

(17) Moffett, R. B.; Rabjohn, N., Eds. *Organic Synthesis*; John Wiley & Sons: New York, 1963; Vol. 4, pp 605–608.

(18) Taguchi, K.; Wesheimer, F. H. *J. Org. Chem.* **1971**, *58*, 556–559.

(19) Love, B. E.; Ren, J. *J. Org. Chem.* **1993**, *58*, 556–559.

(20) Look, G. C.; Murphy, M. M.; Campbell, D. A.; Gallop, M. A. *Tetrahedron Lett.* **1995**, *36*, 2937–2940.

(21) Vaas, R. S.; Duda's, J.; Varma, R. S. *Tetrahedron* **1999**, *40*, 4951–4954.

(22) Billman, J. H.; Tai, K. M. *J. Org. Chem.* **1958**, *23*, 535–539.

(23) White, W. A.; Weingarten, H. *J. Org. Chem.* **1967**, *32*, 213–214.

(24) Weingarten, H.; Chupp, J. P.; White, W. A. *J. Org. Chem.* **1967**, *32*, 3246–3249.

(25) Moretti, I.; Torre, G. *Synthesis* **1970**, 141.

(26) Jennigs, W. B.; Lovely, C. J. *Tetrahedron Lett.* **1988**, *29*, 3725–3728.

(27) Branchaud, B. P. *J. Org. Chem.* **1983**, *48*, 3531–3538.

(28) Liu, G.; Cogan, D. A.; Owens, T. D.; Tang, T. P.; Ellman, J. A. *J. Org. Chem.* **1999**, *64*, 1278–1284.

(29) Jung, D. I.; Choi, T. W.; Kim, Y. Y.; Kim, I. S.; Park, Y. M.; Lee, Y. G.; Jung, D. H. *Synth. Commun.* **1999**, *29*, 1941.

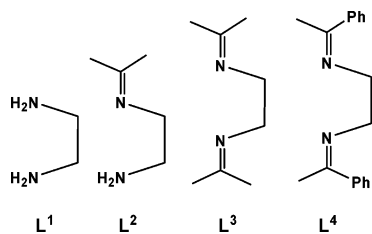
(30) Balakrishna, M. S.; Kaboudin, B. *Tetrahedron* **2001**, *42*, 1127.

(31) Souane, R.; Isel, F.; Peruch, F.; P. J. L. C. R. *Chim.* **2002**, *1*, 43–48.

(32) Jarikote, D. V.; Siddiqui, S. A.; Rajagopal, R.; Thomas, D.; Lahoti, R. J.; Srinivasan, K. V. *Tetrahedron Lett.* **2003**, *44*, 1835.

(33) De, S. K.; Gibbs, R. A. *Tetrahedron Lett.* **2005**, *46*, 1811–1813.

(34) Pozarentzi, M.; Stephanidou-Stephanatou, J.; Tsoleridis, C. A. *Tetrahedron Lett.* **2002**, *43*, 1755–1758.

Scheme 1. Ligands Bound to Thallium Centers

according to this procedure have been reported to present similar preparation conditions and to be extremely moisture sensitive,³⁵ in agreement with the water-scavenging properties of the ligand.³⁶

In this paper we report the unprecedented room-temperature formation of very stable mono- and diimine gold–thallium complexes starting from perhalophenyl ethylenediamine gold–thallium precursors and the study of their reactivity. Their extremely easy formation is illustrated with the complete conversion of the diamine precursors into the diimine ones when the former are exposed to ketone vapors at room temperature.

Results and Discussion

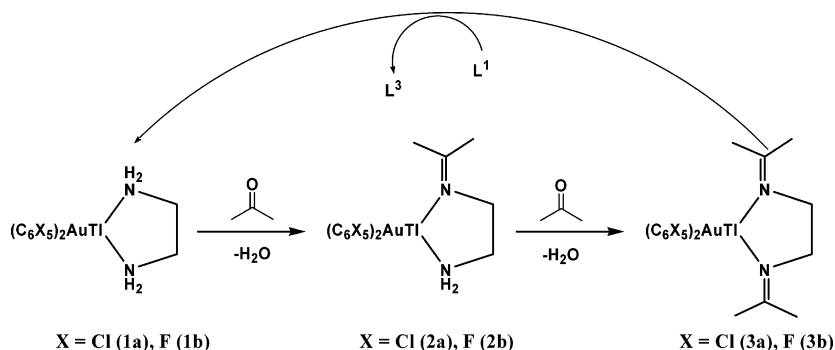
By reacting equimolecular amounts of $[\text{AuTl}(\text{C}_6\text{X}_5)_2]_n$ ($\text{X} = \text{Cl}, \text{F}$) and ethylenediamine two complexes of stoichiometry $[\text{AuTl}(\text{C}_6\text{X}_5)_2(\text{L}^1)]$ ($\text{X} = \text{Cl}, \mathbf{1}$; $\text{F}, \mathbf{1b}$; $\text{L}^1 =$ ethylenediamine) are obtained as white ($\mathbf{1a}$) or green ($\mathbf{1b}$) solids, respectively. Their spectroscopic data are in agreement with the proposed formulation. Thus, their IR spectra in Nujol mulls show, among others, absorptions arising from the C_6Cl_5 ³⁷ and C_6F_5 ³⁸ groups bonded to gold(I) at 837 and 613 for $\mathbf{1a}$ and at 1510, 960, and 768 cm^{-1} for $\mathbf{1b}$, respectively; in the ^1H NMR spectra of both complexes in D_8 -tetrahydrofuran a unique signal appears at similar chemical shift, 2.83 ppm [s, CH_2], due to the equivalent protons of the ethylenediamine groups. Significantly, the position of this resonance differs from that of the free diamine, indicating that this ligand is bonded to thallium even in solution. By contrast, the ^{19}F NMR of complex $\mathbf{1b}$ displays three resonances due to the three types of fluorine atoms of the perhalophenyl groups, which appear at the same chemical shift as in the starting material.³⁹ Elemental analyses and mass spectrometry measurements also agree with these stoichiometries (see Experimental Section).

Reaction of both complexes with ketones in tetrahydrofuran leads to new amine–imine or diimine complexes depending on the stoichiometry (see Scheme 1 (ligands) and Scheme 2). Thus, when we treated complexes $[\text{AuTl}(\text{C}_6\text{X}_5)_2(\text{L}^1)]$ ($\text{X} = \text{Cl}, \mathbf{1a}$; $\text{F}, \mathbf{1b}$) with equimolecular amounts of acetone, the evaporation of the solvent and the addition of dichloromethane led to the complexes $[\text{AuTl}(\text{C}_6\text{X}_5)_2(\text{L}^2)]$ ($\text{X} = \text{Cl}, \mathbf{2a}$; $\text{F}, \mathbf{2b}$), respectively,

in which L^2 is bound to the thallium centers through both types of nitrogen atoms, amine and imine, respectively (see Scheme 2). The analytical and spectroscopic data of both complexes agree with the proposed stoichiometries, and their IR spectra in Nujol mulls show, among others, absorptions arising from the C_6Cl_5 ³⁷ and C_6F_5 ³⁸ groups bonded to gold(I) (see Experimental Section) and bands due to the new ligand (L^2) at 3356, 3296 cm^{-1} [$\nu(\text{N}-\text{H})$] and 1657 cm^{-1} [$\nu(\text{C}=\text{N})$] for $\mathbf{2a}$ and 3380, 3310 cm^{-1} [$\nu(\text{N}-\text{H})$] and 1656 cm^{-1} [$\nu(\text{C}=\text{N})$] for $\mathbf{2b}$. In their ^1H NMR spectra in D_8 -tetrahydrofuran, signals due to methylene groups appear at 2.86 (α position relative to amine group) and 3.47 ppm (β position) for $\mathbf{2a}$ and 2.86 (α position) and 3.48 ppm (β position) for $\mathbf{2b}$. In addition, nonequivalent methyl groups at 1.87 (*endo*) and 1.78 ppm (*exo*) (partially masked by THF residual peak) for $\mathbf{2a}$ and 1.89 (*endo*) and 1.78 ppm (*exo*) for $\mathbf{2b}$ are observed. These spectra seem to indicate the absence of a dissociative equilibrium in solution.

Nevertheless, when the reaction is carried out in a 1:2 (ethylenediamine/acetone) molar ratio, or using acetone as solvent, the complexes obtained are $[\text{AuTl}(\text{C}_6\text{X}_5)_2(\text{L}^3)]$ ($\text{X} = \text{Cl}, \mathbf{3a}$; $\text{F}, \mathbf{3b}$) (Scheme 1), in which the coordination to the thallium atoms takes place by two imine groups. Their IR spectra show absorptions due to the stretching $\nu(\text{C}=\text{N})$, at 1656 cm^{-1} ($\mathbf{3a}$) and 1647, 1632 cm^{-1} ($\mathbf{3b}$), respectively, and those due to the N-H groups of the previously mentioned complexes $\mathbf{2a}$ and $\mathbf{2b}$ disappear. In the ^1H NMR spectra of both complexes in D_8 -tetrahydrofuran two signals arising from the *endo* and *exo* methyl groups and one from the methylene groups at 3.47, 1.88, and 1.81 ppm for $\mathbf{3a}$ and 3.38, 1.92, and 1.85 ppm for $\mathbf{3b}$.

The proposed mechanism for each condensation is likely to be influenced by the acidic characteristics of the thallium centers. Thus, first a nucleophilic attack of the oxygen of the ketone is produced to the thallium center. This attack is favored by the relatively low occupancy of the coordination sphere of the thallium atoms (four positions taking into account the gold interaction, two nitrogen atoms, and the stereochemically active lone pair) (see the crystal structure comments below), as well as by the formal positive charge on these atoms. Subsequently, the transfer of an acidic proton of the amine group to the oxygen center and simultaneous nucleophilic attack of the nitrogen to the carbonyl carbon produces a hemiacetal intermediate that evolves to the imine by β -elimination of water (see Scheme 3). Interestingly, attempts to detect intermediates by NMR experiments at room or at low temperature were unsuccessful, probably because the reaction is faster than the NMR time scale. Nevertheless, a signal at 2.52 ppm due to the water formed in the reaction is observed. Although free ethylenediamine displays in its ^1H NMR spectrum a signal due to the NH_2 groups at 1.22 ppm, in the case of complexes $\mathbf{1a}$, $\mathbf{1b}$, $\mathbf{2a}$, and $\mathbf{2b}$ these groups

Scheme 2. Reactions of $[\text{AuTl}(\text{C}_6\text{X}_5)_2(\text{L}^1)]$ with Acetone

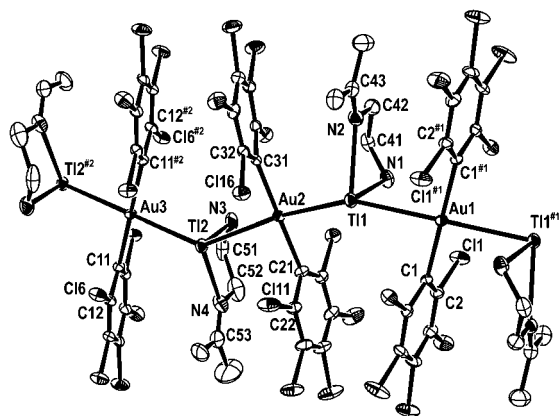
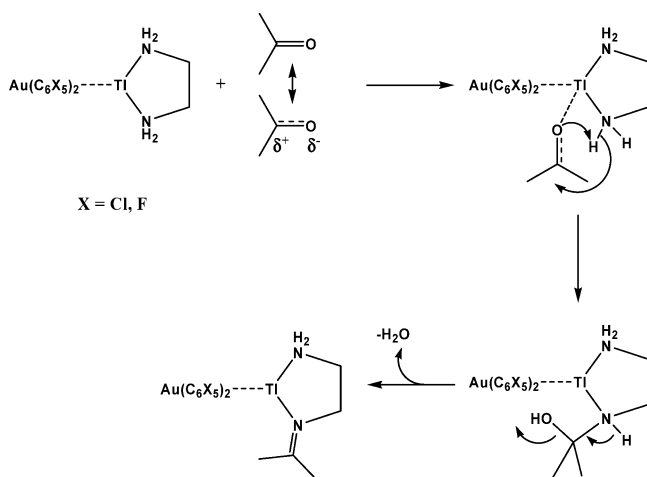


Figure 1. Crystal structure of complex **2a** with the labeling scheme of the atom positions. Hydrogen atoms have been omitted for clarity.

Scheme 3. Proposed Condensation Mechanism



are not observed at the NMR time scale. Nevertheless, their presence is undoubtedly detected in their infrared spectra (see above).

When the starting product is TlPF₆, addition of ethylenediamine in 1:1 molar ratio and subsequent addition of acetone does not produce the formation of the imine, which is perhaps indicative of a certain degree of cooperative interaction between the gold and thallium centers, which modifies the electronic characteristics of the latter, making the reaction possible.

Crystal structures of complexes **2a**, **3a**, and **3b** were determined by X-ray diffraction, and all of them show polymeric chains, which in the case of **3a** runs parallel to the crystallographic *y*-axis, of alternating gold(I) and thallium(I) centers linked via unsupported Au···Tl interactions between 2.9726(3) and 3.1423(19) Å (see Figures 1–3 and Tables 2–4) similar to those observed in other related polynuclear Au/Tl systems with unsupported metal–metal interactions (2.9078(3)–3.3205(3) Å).^{9,10,39–46} They all display square-planar gold(I) centers (taking

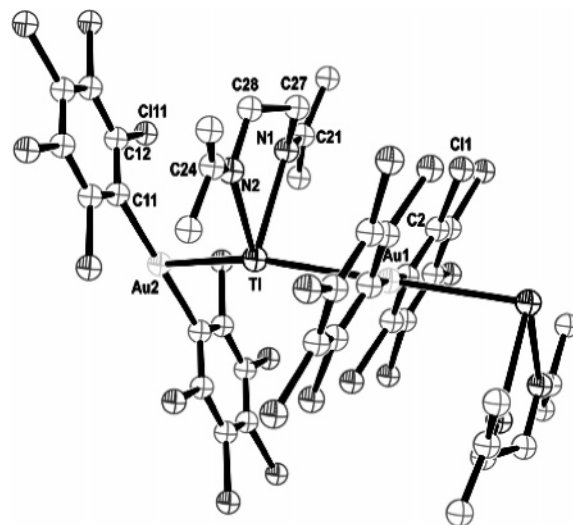


Figure 2. Crystal structure of complex **3a** with the labeling scheme of the atom positions. Hydrogen atoms have been omitted for clarity.

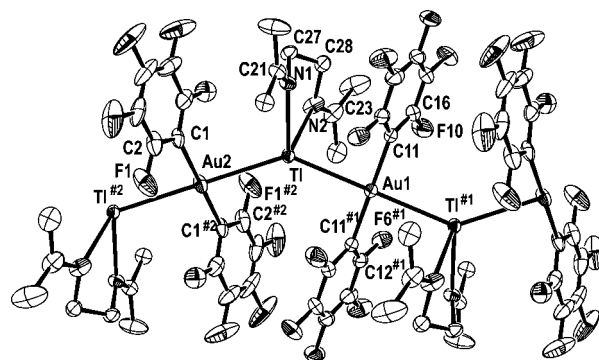


Figure 3. Crystal structure of complex **3b** with the labeling scheme of the atom positions. Hydrogen atoms have been omitted for clarity.

into account the Au···Tl contacts) with typical Au–C bond lengths ranging from 2.038(7) to 2.062(7) Å (see Tables 2–4). Each thallium binds two nitrogen atoms of a chelating amine–imine (**2a**) or diimine ligand (**3a**, **3b**) with slightly longer Tl–N distances for the N atoms of the amine in **2a** (2.675(8) Å) than for the nitrogen centers of the imine groups (Tl–N_{av} = 2.611 Å) in **2a**, **3a**, and **3b**. Nevertheless, they are still longer than the Tl–N bond distances observed in the Tl/Fe complex [(CO)₄Fe(Me₂C=CH₂CH₂CMe₂)₂Fe(CO)₄] (Tl–N_{av} = 2.5475 Å),⁴⁷ which contains the same diimine ligand as **3a** and **3b**, but shorter than most of the Tl–N distances found in other related Au/Tl polymeric systems containing bipy or phen as N-donor ligands (2.641(9)–2.847(5) Å).^{41,44,45} The environment for Tl, considering the intermetallic contacts, is distorted trigonal bipyramidal with a vacant equatorial coordination site apparently associated with the stereochemically active lone pair and the

(35) Paz-Sandoval, M. A.; Domínguez-Durán, M. E.; Pazos-Mayen, C.; Ariza-Castolo, A.; Rosalez-Hoz, M. d. J.; Contreras, R. *J. Org. Chem.* **1995**, *492*, 1–9.

(36) Holm, R. T. *J. Paint Technol.* **1967**, *39*, 385.

(37) Usón, R.; Laguna, A.; Laguna, M.; Manzano, B. R.; Tapia, A. *Inorg. Chim. Acta* **1985**, *151*–153.

(38) Usón, R.; Laguna, A.; Laguna, M.; Manzano, B. R.; Jones, P. G.; Sheldrick, G. M. *Dalton Trans.* **1984**, 285.

(39) Fernández, E. J.; Laguna, A.; López-de-Luzuriaga, J. M.; Monge, M.; Montiel, M.; Olmos, M. E.; Pérez, J. *Organometallics* **2004**, *23*, 774.

(40) Crespo, O.; Fernández, E. J.; Jones, P. G.; Laguna, A.; López-de-Luzuriaga, J. M.; Mendía, A.; Monge, M.; Olmos, M. E. *Chem. Commun.* **1998**, 2233.

(41) Fernández, E. J.; Jones, P. G.; Laguna, A.; López-de-Luzuriaga, J. M.; Monge, M.; Olmos, M. E.; Pérez, J. *Inorg. Chem.* **2002**, *41*, 1056.

(42) Fernández, E. J.; Laguna, A.; López-de-Luzuriaga, J. M.; Mendizábal, F.; Monge, M.; Olmos, M. E.; Pérez, J. *Chem. Eur. J.* **2003**, *9*, 456.

(43) Fernández, E. J.; Laguna, A.; López-de-Luzuriaga, J. M.; Montiel, M.; Olmos, M. E.; Pérez, J. *Organometallics* **2005**, *24*, 1631.

(44) Fernández, E. J.; Laguna, A.; López-de-Luzuriaga, J. M.; Olmos, M. E.; Pérez, J. *Dalton Trans.* **2004**, 1801.

(45) Fernández, E. J.; Jones, P. G.; Laguna, A.; López-de-Luzuriaga, J. M.; Monge, M.; Montiel, M.; Olmos, M. E.; Pérez, J. *Z. Naturforsch.* **2004**, *59b*, 1379.

(46) Fernández, E. J.; Laguna, A.; López-de-Luzuriaga, J. M.; Montiel, M.; Olmos, M. E.; Pérez, J. *Inorg. Chim. Acta* **2005**, *358*, 4293–4300.

(47) van Hal, J. W.; Alemany, L. B.; Whitmire, K. H. *Inorg. Chem.* **1997**, *36*, 3152–3159.

Table 1. Details of Data Collection and Structure Refinement for Complexes 2a, 3a, and 3b

	2a	3a	3b
chemical formula	C ₃₄ H ₂₄ Au ₂ Cl ₂₀ N ₄ Tl ₂	C ₂₀ H ₁₆ AuCl ₁₀ N ₂ Tl	C ₂₀ H ₁₆ AuF ₁₀ N ₂ Tl
cryst color	red	red	yellow
cryst size/mm	0.23 × 0.2 × 0.1	0.15 × 0.1 × 0.08	0.2 × 0.15 × 0.1
cryst syst	triclinic	triclinic	monoclinic
space group	<i>P</i> $\bar{1}$	<i>P</i> $\bar{1}$	<i>P</i> 2 ₁ / <i>c</i>
<i>a</i> /Å	9.2077(1)	11.4427(2)	9.0891(1)
<i>b</i> /Å	15.2963(2)	11.8772(2)	23.9641(4)
<i>c</i> /Å	20.1556(3)	12.8710(2)	11.8157(2)
α /deg	109.814(1)	64.907(1)	90.0
β /deg	93.478(1)	72.058(1)	114.053(1)
γ /deg	103.581(1)	73.161(1)	90.0
<i>U</i> /Å ³	2565.33(6)	1481.23(4)	2350.13(6)
<i>Z</i>	2	2	4
<i>D</i> _c /g cm ⁻³	2.590	2.332	2.475
<i>F</i> (000)	1832	960	1600
<i>T</i> /K	173(2)	173(2)	173(2)
2 θ _{max} /deg	53	56	56
μ (Mo K α)/mm ⁻¹	13.039	11.296	13.173
no. of reflns measd	31 792	17 192	20 523
no. of unique reflns	9661	6927	5564
<i>R</i> _{int}	0.0422	0.0531	0.0355
<i>R</i> ^a (<i>I</i> > 2 σ (<i>I</i>))	0.0334	0.0421	0.0304
<i>wR</i> ^b (<i>F</i> ² , all reflns)	0.0863	0.1118	0.0576
no. of params	575	309	332
no. of restraints	152	74	122
<i>S</i> ^c	1.016	1.036	1.118
max. residual electron density/e ⁻ Å ⁻³	3.070	1.653	0.701

^a $R(F) = \sum ||F_o| - |F_c|| / \sum |F_o|$. ^b $wR(F^2) = [\sum \{w(F_o^2 - F_c^2)^2\} / \sum \{w(F_o^2)^2\}]^{0.5}$; $w^{-1} = \sigma^2(F_o^2) + (aP)^2 + bP$, where $P = [F_o^2 + 2F_c^2]/3$ and a and b are constants adjusted by the program. ^c $S = [\sum \{w(F_o^2 - F_c^2)^2\} / (n - p)]^{0.5}$, where n is the number of data and p the number of parameters.

Table 2. Selected Bond Lengths [Å] and Angles [deg] for Complex 2a^a

Au(1)–C(1)	2.057(7)	Tl(1)–N(2)	2.675(7)
Au(1)–Tl(1)	2.9726(3)	Tl(2)–N(3)	2.520(10)
Au(2)–C(21)	2.056(7)	Tl(2)–N(4)	2.675(8)
Au(2)–C(31)	2.059(7)	N(1)–C(41)	1.452(10)
Au(2)–Tl(2)	2.9571(11)	C(42)–N(2)	1.463(10)
Au(2)–Tl(1)	3.0258(4)	N(2)–C(43)	1.262(11)
Au(3)–C(11)	2.050(6)	N(3)–C(51)	1.455(15)
Au(3)–Tl(2)	3.0365(11)	C(52)–N(4)	1.482(12)
Tl(1)–N(1)	2.618(6)	N(4)–C(53)	1.258(13)
C(1)#1–Au(1)–C(1)	180.0	Au(2)–Tl(2)–Au(3)	139.43(4)
Tl(1)–Au(1)–Tl(1)#1	180.0	C(41)–N(1)–Tl(1)	107.2(5)
C(21)–Au(2)–C(31)	178.9(2)	C(43)–N(2)–C(42)	119.0(7)
Tl(2)–Au(2)–Tl(1)	160.15(2)	C(43)–N(2)–Tl(1)	125.4(6)
C(11)#2–Au(3)–C(11)	180.0	C(42)–N(2)–Tl(1)	114.4(5)
Tl(2)–Au(3)–Tl(2)#2	180.0	C(51)–N(3)–Tl(2)	111.2(6)
N(1)–Tl(1)–N(2)	66.1(2)	C(53)–N(4)–C(52)	121.8(10)
Au(1)–Tl(1)–Au(2)	144.26(1)	C(53)–N(4)–Tl(2)	123.7(7)
N(3)–Tl(2)–N(4)	67.1(3)	C(52)–N(4)–Tl(2)	114.4(7)

^a Symmetry transformations used to generate equivalent atoms: #1 $-x, -y, -z$; #2 $-x-1, -y, -z+1$.

Table 3. Selected Bond Lengths [Å] and Angles [deg] for Complex 3a^a

Au(1)–C(1)	2.041(7)	Tl–N(1)	2.694(9)
Au(1)–Tl	3.0519(3)	N(1)–C(21)	1.230(19)
Au(2)–C(11)	2.062(7)	N(1)–C(27)	1.56(2)
Au(2)–Tl	3.0877(3)	N(2)–C(24)	1.247(19)
Tl–N(2)	2.641(10)	N(2)–C(28)	1.45(2)
C(1)#1–Au(1)–C(1)	180.0	Tl#2–Au(2)–Tl	180.0
Tl–Au(1)–Tl#1	180.0	N(2)–Tl–N(1)	68.5(4)
C(11)#2–Au(2)–C(11)	180.0	Au(1)–Tl–Au(2)	150.59(1)

^a Symmetry transformations used to generate equivalent atoms: #1 $-x+1, -y+1, -z$; #2 $-x+1, -y, -z$.

gold centers occupying the apical positions (Au–Tl–Au angles from 139.20(1)° to 150.59(1)°).

Finally, in complex **2a**, a series of N–H \cdots Cl hydrogen bonds are present between atoms of the same polymeric chain (see

Table 4. Selected Bond Lengths [Å] and Angles [deg] for Complex 3b^a

Tl–N(2)	2.591(5)	N(1)–C(21)	1.264(7)
Tl–N(1)	2.603(5)	N(1)–C(27B)	1.476(16)
Tl–Au(1)	3.04792(19)	N(1)–C(27A)	1.517(15)
Tl–Au(2)	3.14273(19)	N(2)–C(23)	1.274(8)
Au(1)–C(11)	2.045(6)	N(2)–C(28B)	1.419(13)
Au(2)–C(1)	2.047(6)	N(2)–C(28A)	1.608(15)
N(2)–Tl–N(1)	67.17(16)	C(21)–N(1)–Tl	126.1(4)
Au(1)–Tl–Au(2)	139.204(7)	C(27B)–N(1)–Tl	110.2(7)
C(11)–Au(1)–C(11)#1	180.0	C(27A)–N(1)–Tl	113.5(7)
Tl–Au(1)–Tl#1	180.0	C(23)–N(2)–C(28B)	124.0(7)
C(1)–Au(2)–C(1)#2	180.0	C(23)–N(2)–C(28A)	114.2(7)
Tl–Au(2)–Tl#2	180.0	C(23)–N(2)–Tl	125.8(5)
C(21)–N(1)–C(27B)	122.8(8)	C(28B)–N(2)–Tl	109.7(5)
C(21)–N(1)–C(27A)	118.2(8)	C(28A)–N(2)–Tl	112.4(5)

^a Symmetry transformations used to generate equivalent atoms: #1 $-x+1, -y, -z+1$; #2 $-x+2, -y, -z+2$.

Table 5. Hydrogen Bonds for Complex 2a [Å and deg]^a

D–H \cdots A	<i>d</i> (D–H)	<i>d</i> (H \cdots A)	<i>d</i> (D \cdots A)	\angle (DHA)
N(1)–H(1A) \cdots Cl(5)#1	0.92	2.72	3.625(7)	167.8
N(1)–H(1B) \cdots Cl(15)	0.92	2.73	3.530(7)	145.3
N(3)–H(3A) \cdots Cl(20)	0.92	2.96	3.410(10)	112.1
N(3)–H(3B) \cdots Cl(15)	0.92	2.68	3.579(8)	164.1

^a Symmetry transformations used to generate equivalent atoms: #1 $-x, -y, -z$.

Table 5), which may contribute to the stabilization of the system, but do not give rise to two- or three-dimensional arrays.

The crystal structure of complex **1a** was also determined by X-ray diffraction methods (see Supporting Information), although the crystals were not good enough to give the desired degree of accuracy and the thallium center is also disordered over two different positions (75:25). It consists of discrete dinuclear molecules [AuTl(C₆Cl₅)₂(L¹)] with an intramolecular Au–Tl distance of approximately 3.1 Å and an intermolecular Au–Tl distance of \sim 4.04 Å with the neighboring molecules,

giving rise to a “discontinuous polymer” extended parallel to the crystallographic *y*-axis.

Different results are obtained when the precursor gold–thallium ethylenediamine complexes **1a** and **1b** react with the stronger acceptor acetophenone, because they both lead to the double imine formation L^4 (see Scheme 1), independently of the molar ratio employed, 1:1 (as in complexes **2a** and **2b**) or 1:2 (as in complexes **3a** and **3b**). Consequently, when the reactions are carried out in a 1:1 molar ratio, complexes **4a,b** and unreacted **1a,b** are isolated from the reaction medium. However, when the stoichiometry is 1:2, complexes **4a** and **4b** are obtained as the only products in higher yields.

As before, their analytical and spectroscopic data are also in accordance with the proposed stoichiometry, $[AuTl(C_6X_5)_2(L^4)]_n$, and, for instance, their IR spectra show only absorptions due to the stretching $C=N$ vibrations and the ^{19}F NMR spectrum of **4a** shows three resonances due to the three types of fluorine atoms of the perfluorophenyl groups at a chemical shift similar to that in the starting material. Interestingly, in the 1H NMR spectra of **4a** and **4b** signals due to the methyl, phenyl, and methylene groups appear at different chemical shifts than those observed for the free ligand (7.86–7.29 (10H, Ph), 3.86 (s, 4H, CH_2), 2.25 (s, 6H, CH_3) in THF-*D*₈), indicating the coordination of the thallium center in the same way as the commented ethylenediamine in the precursor complexes. However, the spectra show only signals corresponding to one isomer of the ligand, which indicates that, as in the other complexes, there is no dissociative equilibrium in solution. The data also show that all the methyl protons are equivalent (see Experimental Section), suggesting the *cis* disposition of the substituents. NMR studies of a molybdenum complex about the disposition of these groups inward toward or outward from the coordination sphere of the metal center suggest that in this case the chemical shifts of the methyl groups are in agreement with their inward disposition.³⁵ This proposal with the smaller methyl groups situated toward the thallium center seems to be in agreement with the suggested mechanism in that, first, the condensation is produced with the diamine ligand bonded to the thallium center and, second, the $[Au(C_6X_5)_2]^-$ groups probably interact with the thallium atoms since the bulkier phenyl groups lie at the less sterically hindered positions.

Very interestingly, the ethylenediamine complexes **1a** and **1b** can also react in the solid state with ketone vapors at room temperature. The transformation of the ethylenediamine complexes in the corresponding diimine ones takes place in a few seconds (about 10 s) when a flask containing $[AuTl(C_6X_5)_2(en)]$ ($X = Cl$, **1a**; F , **1b**) is subjected to a saturated atmosphere of the ketone. Thus, a very rapid change of color of the solids from white (**1a**) to red (acetone) or orange (acetophenone) and from green (**1b**) to yellow for both ketones is observed (see Figure 4). A detailed observation of the photograph that shows several moments of the transformation indicates a change from green $[AuTl(C_6F_5)_2(L^1)]$, **1b**, to orange and yellow. These colors are similar to those observed for the solids $[AuTl(C_6F_5)_2(L^2)]_n$, **2b**, and $[AuTl(C_6F_5)_2(L^3)]_n$, **3b**, respectively, which could indicate that the conversion is produced in two steps. The study of this process for complex **1b** by infrared spectroscopy in the solid state agrees with this assumption. Thus, the intensities of the original bands of the ethylenediamine complex, placed at 3388 and 3322 cm^{-1} , decrease as the new ones, at 3380, 3310, and 1656 cm^{-1} , due to amine $\nu(N-H)$ and imine $\nu(C=N)$, increase. These appear at wavenumbers similar to those in $[AuTl(C_6F_5)_2(L^2)]_n$, **2b**. The conversion to the double imine complex does not begin until the first condensation has been

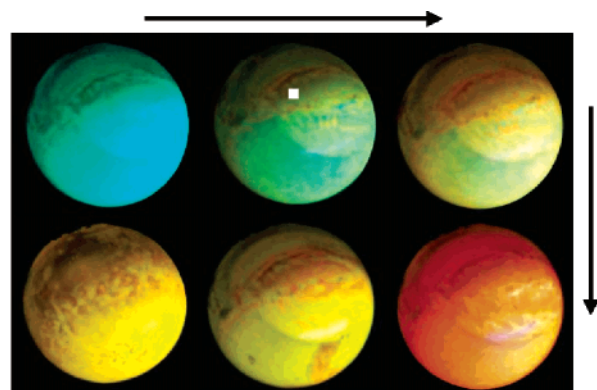


Figure 4. Photograph showing the sequence of the transformation of a powder sample of compound $[AuTl(C_6F_5)_2(L^1)]$, **1b** (upper left), deposited in a flask and subjected to acetone vapors. The arrows indicate the steps of the conversion.

produced. Thus, bands at 1647 and 1632 cm^{-1} , corresponding to the second condensation, appear and their intensity increase at the same time as the previous bands, at 3380, 3310 and 1656 cm^{-1} , diminish. Significantly, bands assigned to the three complexes do not coexist at the same time in any moment of the process.

Similarly, complex **1a** follows similar exchange and the final solid does not show bands due to the remaining amine $\nu(N-H)$ vibrations, and instead, the expected $\nu(C=N)$ appears. Also the 1H NMR and mass spectra do not show any evidence of the presence of starting materials, indicating a complete conversion into the diimine products. As in the solids obtained in solution, these materials are stable to air and moisture indefinitely, in contrast to other reported imine complexes, whose stability to moisture is very low.^{35,47} This behavior could perhaps make these diamine products appropriate for their use as irreversible sensors of ketone groups, for instance, in the food industry.

Addition of ethylenediamine to a solution of the diimine complexes **3a,b** and **4a,b** leads to the displacement of the diimine ligand by the diamine one and formation of the starting products **1a,b** quantitatively. In the case of complexes **3a,b**, addition of ethylenediamine allows us to identify in the solution the precursors ethylenediamine and acetone, while in the case of the complexes **4a,b** the more stable $PhMeC=N(CH_2)_2N=CMePh$ (L^4) evolves only to the decomposition products amine and acetone by the presence of water in the reaction medium. This result agrees with the data obtained from the mass spectra of the diimine derivatives, in which for **3a,b** no peak due to the isolated diimine L^3 is found, while in the case of **4a,b** a peak at $m/z = 265$ corresponding to $[L^4+H]^+$ appears. In this case, this synthetic pathway can be used for the easy formation of this imine ligand by displacement with ethylenediamine and, thus, recovering the starting product, which, to some extent, can be considered a catalytic cycle.

Finally, as can be expected from their structures and colors under visible radiation, all the complexes exhibit a bright luminescence in the solid state (see Supporting Information), but not in deoxygenated tetrahydrofuran solutions, where, in addition, their absorption spectra display only high-energy structureless absorptions assigned to the perhalophenyl rings.^{43,46} Thus, they show single emissions at 515 (exc. 395) **1a**, 505 (exc. 430) **1b**, 670 (exc. 510) **2a**, 625 (exc. 515) **2b**, 640 (exc. 540) **3a**, 675 (exc. 455) **3b**, 560 (exc. 360) **4a**, and 575 nm (exc. 465 nm) **4b** at room temperature. The assignment of the excited states responsible for the luminescence in these complexes is made on the basis of similar extended heteropoly-

nuclear gold–thallium chains prepared in this laboratory with similar^{44,45} or different¹⁰ donor centers, and therefore, we assign them to delocalized excitons along the heterometallic chains influenced by the coordination environment of the thallium centers.

Further studies of the gold–thallium precursors in solution with different donor–acceptor amines and ketones in order to obtain imine ligands, including those whose preparation requires very strong reaction conditions, as well as in solid/vapor media, to test the capabilities of these materials for sensing applications are now under current research in this laboratory.

Experimental Section

Instrumentation. Infrared spectra were recorded in the range 4000–200 cm⁻¹ on a Perkin-Elmer FT-IR Spectrum 1000 spectrophotometer using Nujol mulls between polyethylene sheets. C, H, S analyses were carried out with a Perkin-Elmer 240C microanalyzer. Mass spectra were recorded on a HP59987 A electrospray. ¹H and ¹⁹F NMR spectra were recorded on a Bruker ARX 300 in D₈-THF solutions. Chemical shifts are quoted relative to SiMe₄ (¹H, external) and CFCl₃ (¹⁹F, external). UV–visible absorption spectra were obtained on a Hewlett-Packard 8453 diode array UV–visible spectrophotometer in tetrahydrofuran solutions (1 × 10⁻⁵ M). Corrected excitation and emission spectra were recorded with a Jobin-Yvon Horiba Fluorolog 3-22 Tau-3 spectrofluorimeter.

General Comments. Ethylenediamine, acetone, and acetophenone are commercially available and were purchased from Aldrich. The precursor complexes [AuTl(C₆F₅)₂]³⁹ and [AuTl(C₆Cl₅)₂]⁹ were obtained according to literature procedures. **CAUTION:** Thallium salts have been found to be toxic to living organisms.

Preparation of [AuTl(C₆X₅)₂(L¹)]_n (X = Cl (1a**), F (**1b**)).** To a tetrahydrofuran solution (20 mL) of [AuTl(C₆X₅)₂]_n (0.20 mmol; 180 mg for X = Cl, 147 mg for X = F) was added ethylenediamine (0.20 mmol, 14 μL). The solution was stirred for 10 min, and the solvent was removed under reduced pressure. The addition of dichloromethane gave a white precipitate for **1a** and green for **1b**. The solids were filtered off and washed with dichloromethane (3 × 5 mL). Yield: 92% for **1a** and 87% for **1b**. Anal. (%) Calcd for **1a** (C₁₄H₈AuCl₁₀N₂Tl): C, 17.51; H, 0.84; N, 2.92. Found: C, 17.52; H, 0.84; N, 2.91; for **1b** (C₁₄H₈AuF₁₀N₂Tl): C, 21.14; H, 1.01; N, 3.52. Found: C, 21.19; H, 1.01; N, 3.52. FT-IR (Nujol mulls): ν(C₆Cl₅) at 837 and 613 cm⁻¹, ν(N–H st) at 3365 and 3290 cm⁻¹ for **1a**; ν(C₆F₅) at 1510, 960, and 768 cm⁻¹, ν(N–H st) at 3388 and 3322 cm⁻¹ for **1b**. ¹H NMR (THF-D₈, room temperature, ppm): δ 2.83 (s, CH₂) for **1a** and 2.83 (s, CH₂) for **1b**. ¹⁹F NMR (THF-D₈, room temperature, ppm): δ -114.9 (m, 2F, F_o); δ -163.3 (t, 1F, F_p, ³J(F_p–F_m) = 18.8 Hz); δ -164.4 (m, 2F, F_m) for **1b**. ES(+) *m/z*: 263/265 [Tl(en)]⁺. ES(-) *m/z*: 695 [Au(C₆Cl₅)₂]⁻ for **1a** and 531 [Au(C₆F₅)₂]⁻ for **1b**.

Preparation of [AuTl(C₆X₅)₂(L²)]_n (X = Cl (2a**), F (**2b**)).** Two solutions of [AuTl(C₆X₅)₂(L¹)] (0.20 mmol; 192 mg for X = Cl, 159 mg for X = F) in 20 mL of tetrahydrofuran were treated with acetone (0.20 mmol, 15 μL) and stirred at room temperature. After 5 min, the evaporation of the solvent and the addition of dichloromethane give an orange precipitate in both cases. The solids were filtered off and washed with dichloromethane (3 × 5 mL). Yield: 75% for **2a** and 82% for **2b**. Anal. (%) Calcd for **2a** (C₁₇H₁₂-AuCl₁₀N₂Tl): C, 20.42; H, 1.21; N, 2.80. Found: C, 20.43; H, 1.20; N, 2.80; for **2b** (C₁₇H₁₂AuF₁₀N₂Tl): C, 24.44; H, 1.45; N, 3.35. Found: C, 24.40; H, 1.45; N, 3.36. FT-IR (Nujol mulls): ν(C₆-Cl₅) at 834 and 605 cm⁻¹, ν(N–H st) at 3356 and 3296 cm⁻¹, ν(C=N st) 1657 cm⁻¹ for **2a**; ν(C₆F₅) at 1502, 955, and 787 cm⁻¹, ν(N–H st) at 3380 and 3310 cm⁻¹, ν(C=N st) 1656 cm⁻¹ for **2b**. ¹H NMR (THF-D₈, room temperature, ppm): 2.86 (s, 2H, α-CH₂), 3.47 (s, 2H, β-CH₂), 1.87 (s, 3H, CH₃), 1.78 (s, 3H, CH₃) for **2a**

and 2.86 (s, 2H, α-CH₂), 3.48 (s, 2H, β-CH₂), 1.89 (s, 6H, CH₃), 1.78 (s, 3H, CH₃) for **2b**. ES(+) *m/z*: 203/205 [Ti]⁺, 263/265 [Ti(en)]⁺ for **2b**. ES(-) *m/z*: 695 [Au(C₆Cl₅)₂]⁻ for **2a** and 531 [Au(C₆F₅)₂]⁻ for **2b**.

Preparation of [AuTl(C₆X₅)₂(L³)]_n (X = Cl (3a**), F (**3b**)).** Two solutions of [AuTl(C₆X₅)₂(L¹)] (0.20 mmol; 192 mg for X = Cl, 159 mg for X = F) in 20 mL of tetrahydrofuran were treated with acetone (0.40 mmol, 29 μL) and stirred at room temperature. After 5 min, the evaporation of the solvent and the addition of dichloromethane give a red precipitate for **3a** and yellow for **3b**. The solids were filtered off and washed with dichloromethane (3 × 5 mL). Yield: 78% for **3a** and 87% for **3b**. Anal. (%) Calcd for **3a** (C₂₀H₁₆AuCl₁₀N₂Tl): C, 23.09; H, 1.55; N, 2.69. Found: C, 23.06; H, 1.55; N, 2.70; for **3b** (C₂₀H₁₆AuF₁₀N₂Tl): C, 27.43; H, 1.84; N, 3.20. Found: C, 27.34; H, 1.86; N, 3.21. FT-IR (Nujol mulls): ν(C₆Cl₅) at 836 and 616 cm⁻¹, ν(C=N st) 1656 cm⁻¹ for **3a**; ν(C₆F₅) at 1502, 957, and 783 cm⁻¹, ν(C=N st) 1647 and 1632 cm⁻¹ for **3b**. ¹H NMR (THF-D₈, room temperature, ppm): 3.47 (s, 4H, CH₂), 1.88 (s, 6H, CH₃), 1.81 (s, 6H, CH₃) for **3a** and 3.38 (s, 4H, CH₂), 1.92 (s, 6H, CH₃), 1.85 (s, 6H, CH₃) for **3b**. ES(+) *m/z*: 203/205 [Ti]⁺, 483/485 [Ti(L³)₂]⁺ for **3b**. ES(-) *m/z*: 695 [Au(C₆Cl₅)₂]⁻ for **3a** and 531 [Au(C₆F₅)₂]⁻ for **3b**.

Preparation of [AuTl(C₆X₅)₂(L⁴)]_n (X = Cl (4a**), F (**4b**)).** Two solutions of [AuTl(C₆X₅)₂(L¹)] (0.20 mmol; 192 mg for X = Cl, 159 mg for X = F) in 20 mL of tetrahydrofuran were treated with acetophenone (0.40 mmol, 47 μL) and stirred at room temperature. After 5 min, the evaporation of the solvent and the addition of dichloromethane give an orange precipitate for **4a** and yellow for **4b**. The solids were filtered off and washed with dichloromethane (3 × 5 mL). Yield: 65% for **4a** and 76% for **4b**. Anal. (%) Calcd for **4a** (C₃₀H₂₀AuCl₁₀N₂Tl): C, 30.95; H, 1.73; N, 2.41. Found: C, 30.84; H, 1.76; N, 2.42; for **4b** (C₃₀H₂₀AuF₁₀N₂Tl): C, 36.04; H, 2.02; N, 2.80. Found: C, 35.97; H, 2.04; N, 2.79. FT-IR (Nujol mulls): ν(C₆Cl₅) at 833 and 610 cm⁻¹, ν(C=N st) 1633 cm⁻¹ for **4a**; ν(C₆F₅) at 1497, 960, and 758 cm⁻¹, ν(C=N st) 1621 cm⁻¹ for **4b**. ¹H NMR (THF-D₈, room temperature, ppm): 7.63–7.32 (10H, Ph), 3.89 (s, 4H, CH₂), 2.33 (s, 6H, CH₃) for **4a** and 7.67–7.36 (10H, Ph), 3.89 (s, 4H, CH₂), 2.33 (s, 6H, CH₃) for **4b**. ES(+) *m/z*: 203/205 [Ti]⁺, 265 [L⁴+H]⁺. ES(-) *m/z*: 695 [Au(C₆Cl₅)₂]⁻ for **4a** and 531 [Au(C₆F₅)₂]⁻ for **4b**.

Crystallography. The crystals were mounted in inert oil on glass fibers and transferred to the cold gas stream of a Nonius Kappa CCD diffractometer equipped with an Oxford Instruments low-temperature attachment. Data were collected by monochromated Mo Kα radiation (λ = 0.71073 Å). Scan type: ω and φ. Absorption corrections: numerical (based on multiple scans). The structures were solved by direct methods and refined on F² using the program SHELXL-97.⁴⁸ All non-hydrogen atoms were anisotropically refined, and hydrogen atoms were included using a riding model. Further details on the data collection and refinement methods can be found in Table 1. Selected bond lengths and angles are shown in Tables 2–4, and crystal structures of **2a**, **3a**, and **3b** can be seen in Figures 1–3. CCDC-291380–291382 contain the supplementary crystallographic data for this paper. These data can be obtained free of charge via www.ccdc.cam.ac.uk/conts/retrieving.html (or from the Cambridge Crystallographic Data Center, 12 Union Road, Cambridge CB2 1EZ, UK; fax: (+44) 1223-336-033; or e-mail: deposit@ccdc.cam.ac.uk).

Special Details. In compound **2a** Tl(2) is disordered over two different positions (75:25). For this reason its bond lengths and angles are referred to the thallium atom with higher occupancy. In complex **3b** the methylenic carbon atoms of one of the diimine ligands (C(27) and C(28)) are disordered over two different positions (50:50).

(48) Sheldrick, G. M. *SHELXL-97*; University of Göttingen: Göttingen, Germany, 1997.

Acknowledgment. This work was supported by the DGI-(MEC)/FEDER (CTQ2004-05495). M.M. thanks CAR for a grant.

Supporting Information Available: Tables S1 and S2 show details of data collection, structure refinement, and selected bond lengths and angles for complex **1a**. Figure S1 shows the molecular

structure of this complex. Figure S2 shows the emission spectra in the solid state of the complexes **1a–4a** and **1b–4b**. Figures S3–S8 display the structures of **2a**, **3a** and **3b** viewed perpendicular and parallel to the polymetallic chains. This material can be obtained, free of charge, via the Internet at <http://pubs.acs.org>.

OM051030J